

SUBSURFACE BIOIMAGING USING ANGULAR DOMAIN OPTICAL BACKSCATTERING ILLUMINATION

F. Vasefi, P.K.Y. Chan, B. Kaminska, and G. H. Chapman

Computational and Integrative Bio-Engineering Research, [CIBER](#)
Simon Fraser University, School of Engineering Science, 8888 University Drive,
Burnaby, B.C., Canada V5A 1S6

Abstract— While Coherence or Time Domain Optical tomography within highly scattering media observes the shortest path photons over the dominant randomly scattered background light, Backscattering Angular Domain Imaging employs micromachined collimators to detect photons within small angles of laser light reflected from the high scattering medium. These angular filters are composed of micromachined semicircular silicon collimator channels. By illuminating from the front side phantom test objects were observed in scattering media up to 3 mm deep in the medium at effective scattered to ballistic ratios from 1:1 to greater than 3E12:1. Results from carbon coating the collimators using a sputtering system to decrease internal reflectivity are shown.

Keywords: *Optical tomography, angular domain imaging, backscattering, silicon micromachined collimating array (SMCA), carbon coating*

I. INTRODUCTION

Diagnostic medical imaging is now a fundamental part of the practice of modern medicine. The major modalities include: X-ray (planar and Computed Tomography - CT), ultrasound, nuclear (planar, Positron Emission Tomography - PET, and Single Photon Emission Computed Tomography - SPECT), and magnetic resonance (MR).

Optical imaging is a method that utilizes the spatial variation in the optical properties of a biospecie whether a cell, a tissue, an organ, or an entire live specimen. These optical properties include reflection, scattering, absorption, and fluorescence.. Techniques relying on ionizing radiation (e.g. X-ray, CT, SPECT, PET) subject the patient to a radiation dose that carries a small but finite potential detriment. This places a limit on their usage, particularly in the cases of pregnant women and children. In contrast, optical imaging, ultrasound and MR imaging do not carry these risks [1].

Medical optical tomography techniques [2] are based on the fact that light can penetrate quite deeply into tissue where it is mostly scattered, though a very small proportion is absorbed. The amount of optical absorption is directly related to the chemical composition of the tissue and the wavelength of the light source. The optical scattering coefficient is related to the morphology and refractive index distribution of the tissue composition. The cell, nucleus, and other organelles contribute to the tissue scattering property [3].

Biological tissues with abnormal physiological attributes have different tissue compositions, and these differences can make them noticeable in the form of different optical absorption and scattering properties [4]. The major challenge faced by optical imaging in biological tissue is extremely high levels of scattering. The scattering coefficients of biological tissues range from 10 cm^{-1} to $>100 \text{ cm}^{-1}$, with total scattering being *exponentially* related to the scattering coefficient. At such high scattering coefficients, the majority of the photons follow random-walk-like trajectories within tissue of a centimeter or greater thickness. The key issue to successful optical imaging is separating the components of the light into unscattered (ballistic) or minimally scattered (quasi-ballistic) light versus highly scattered light. The first component carries information about the structure of the tissue through which it passes, but is many orders of magnitude smaller than the second component (i.e. highly scattered light). This makes optical imaging more difficult than most other medical imaging modalities such as X-ray imaging, in which the photons travel through the tissue in a ballistic trajectory. As a result, it is challenging for purely optical imaging to achieve clinically feasible imaging resolution. In our previous works [1, 10], Angular Domain Imaging (ADI) tomography was introduced as an optical imaging modality. In this paper we investigate the use ADI with illumination of scattering media on the same side as the detector. This simulates detection of features within a few millimeters of the surface tissue, such as subcutaneous applications.

II. BACKGROUND

A number of optical imaging techniques have been proposed and studied in the past decade. These methods can be divided into three classes that will be explained in this section.

The time-gated optical imaging [5,6] and optical coherence tomography [7] are both dependent on the *path length* of the photon. Time Domain Tomography, which measures transmitted light generated by femtosecond laser pulses and looks for the earliest arriving photons [6]. The ballistic/quasiballistic photons arrive first, having traveled the shortest distance, while scattered photons arrive later. Another technique is called Optical Coherence Tomography [7] that directs a reference beam to a detector at the system output to measure only photons in phase with the source

beam, since the chaotic paths of scattered light generate random phases. Both techniques have successfully imaged objects buried inside thick tissue, but both methods have the disadvantage of requiring very expensive equipment and complex, sensitive setups.

The second optical imaging method is called *diffused/transport model based optical imaging*, which includes frequency domain optical imaging [8] and DC diffuse tomography [9]. Various sophisticated image reconstruction algorithms based on diffuse equation or transport equation are still under research in these methods to reconstruct the original object image. The image quality is usually algorithm dependent and the spatial resolution is rather poor.

The third method is Angular Domain Imaging that employs micromachined collimators detecting photons within small angles of aligned laser light sources. These angular filters are micromachined silicon collimator channels in microns range wide by with longer length to gain high aspect ratio, giving a tiny acceptance angle behind a CMOS detector array as shown in Figure 1 [1,10]. This method of optical imaging is the one upon which the proposed method of this research is based as explained in the next section.

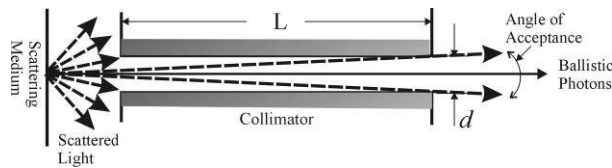


Figure 1. Collimator separation of Ballistic and Scattered light

Another classification of optical imaging is based on the position of light source and the optical detector [15]. Light source can be on the same side as a detector or on the opposite side. Transillumination microscopic imaging is based on the direct light propagation through a tissue. The previously reported ADI research has employed transillumination methods and targets the imaging through modestly thick (few cm) scattering media.

When the light source and the detector are both on the same side of a tissue, the tissue imaging can come from reflection or backward scattering of the light. In this paper we demonstrate the use of a front illumination source to create a scattering light source beneath the surface of the scattering medium. We then use Angular Domain Imaging to detect objects within near surface of the scattering media illuminated by that scattering source.

III. METHOD

A. Fabrication of the Silicon Micromachined Collimating Array

To obtain fine object resolution and detection, a collimating array must have relatively small holes with small spacing between them. In our design, as shown in Figure 2, we used 51 μm diameter holes with 102 μm spacing to

produce a parallel array of collimators with a predicted object resolution in the 100-200 μm range.

To observe an image, this collimator was aligned to a CMOS imaging array detector in such a way that the hole spacings of 102 μm matched the spacing requirement to be integer numbers of the CMOS detector. Each block of grooves covered 20 X 10 mm squares, fabricated on a 100 mm wafer. When combined with an encasement, these grooves became the Silicon Micromachined Collimator Array (SMCA), which had a very high aspect ratio (200:1) resulting in a small angle of acceptance (0.29°). The large length of the array (10 mm) combined with the small hole size suggested that silicon surface micromachining could best generate the structure. For these initial experiments, only a linear collimating array was created.

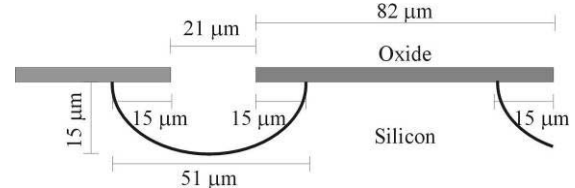


Figure 2. SMCA Masked layer to get 51 μm holes on 102 μm centers

The basic steps of the collimator microfabrication are shown in detail in [1,10]. These collimators started with a furnace $\langle 100 \rangle$ silicon wafer oxidation (0.5 μm thick) which is then photolithographically patterned and etched with HF to create the masking layer of the collimator grooves (see Figure 2). The silicon was etched in HF, HNO_3 , CH_3COOH [10] using the oxide openings to produce a groove width of 51 μm after isotropic etching, with a 15 μm undercut on each channel side (see Figure 2). The oxide was then stripped leaving the grooved structure.

In one set of experiments the microchannel array have been coated with a thin layer of carbon ($\sim 200\text{nm}$) in sputtering deposition system, as shown in Figure 3, in order to get better attenuation from the light reflected from the channel walls. The carbon deposited on the bottom and also on the side wall are approximately 75% and 50% of the thickness of carbon at the top edge respectively (Figure 3). After fabrication, the wafer was cleaved into 20 x 10 mm sections along the cutting grooves between each section. For the first setup, a carbon coated silicon wafer was bonded to the etched wafer top, creating tubes in the collimator with half-circular cross-sections as can be seen in Figure 4.

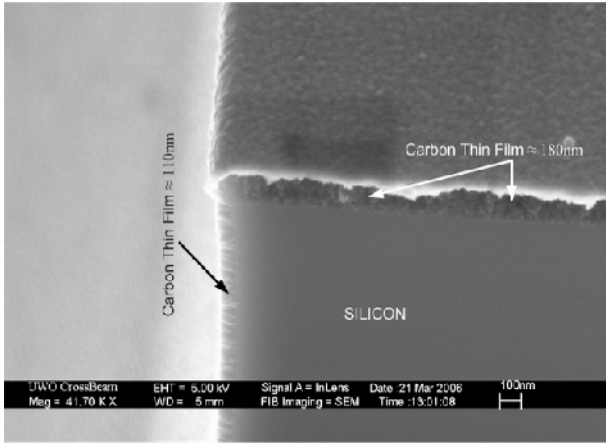


Figure 3. The edge analysis of the Silicon Micromachined Collimating Array with thin layer of carbon.

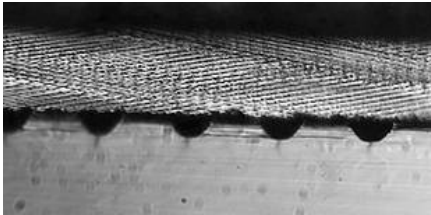


Figure 4. Bonding of a cover chip to the etched section to create the Silicon Micromachined Collimating Array.

B. Backscattering angular domain imaging operation

Generally, light entering the tissue undergoes both absorption and scattering. In its simplest form, the laser beam intensity follows an exponentially decaying Beer-Lambert law along its path through the media:

$$I_{out} = I_{in} \exp[-(\mu_a + \mu_s)d] = I_{in} \exp[-\mu_{eff}d] \quad (1)$$

where, for typical mammography values, the absorption coefficient is $\mu_a = 0.7 \text{ cm}^{-1}$, the scattering coefficient $\mu_s = 130 \text{ cm}^{-1}$ and the depth is $d = 5 \text{ cm}$ [11]. Light which is unscattered becomes “Ballistic Photons.” For this example, the ratio of scattered to ballistic photons is $6.7 \times 10^{283}:1$. Fortunately, most of the light is not scattered uniformly in all directions, but instead tends to divert mostly towards the laser beam’s direction of motion. The measurements are characterized using the Scattering Ratio SR (ratio of scattered to unscattered light):

$$SR = \frac{I_0}{I_{bq}} - 1 \quad (2)$$

where I_0 is the initial light intensity and I_{bq} is the combined ballistic and quasi-ballistic light intensity.

This forward scattering creates an effective absorption anisotropic coefficient [10], $\mu_{eff} = 4.2 \text{ cm}^{-1}$ for the so called “quasiballistic or snake photons” (ones that are mostly scattered forward). Since these quasiballistic photons also contain desired optical information, their scattering ratio of about $10^{11}:1$ represents a significant target for detection in this research.

If a photon emerges from a scattering medium with an angle greater than the acceptance angle then it either fails to enter the collimator or becomes absorbed within it (Figure 1). Hence, in transillumination ADI only the ballistic and quasiballistic photons will be detected. this technique greatly enhanced detection competing with existing optical imaging methods but with *a much simpler detection system* [1,10].

Test phantoms used for this research are placed in a container holding a liquid scattering medium. The test objects are located at various positions within the container. To measure the resolution of the system, aluminum thin film on glass substrate phantoms, shown in Figure 5, were fabricated using photolithography consisting of parallel lines and spaces of $51 \mu\text{m}$, $102 \mu\text{m}$, $153 \mu\text{m}$, and $204 \mu\text{m}$ line widths.

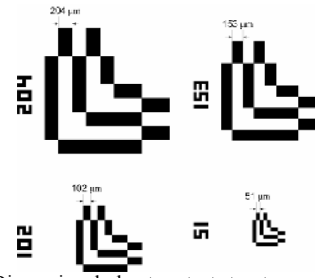


Figure 5. Two-Dimensional phantom test structures

Previous Angular Domain Imaging experiments [1] have focused on using a laser source aligned to the collimating array for the maximum depth penetration with transillumination in the turbid medium. However, the same technique will work, though at much lower total scattering, if the light source is not aligned to the collimator. This allows detection of objects at moderately shallow depths by illumination from the front (i.e. the same side as the collimator [1]). The experiments were undertaken with angled illumination of the scattering medium, as shown in the setup on Figure 6. As the laser beam penetrates into the turbid medium, it undergoes an extremely high number of scattering events. This randomly scattered light creates an approximate sphere of illumination below the surface. This sphere acts as a subsurface light source to illuminate the objects between the sphere of illumination and the collimator. (see figure 6). To create an easily controllable scattering medium, a solution was created by mixing specific amounts of 2% partially skimmed milk with de-ionized (DI) water to achieve a desired scattering level. Milk was chosen as it has properties similar to tissue and exhibits good scattering characteristics and a low absorption coefficient. The principal here is that the scattered light that starts out aligned to the collimator will have the highest probability of being detected provided it is not scattered by the medium or blocked by the test objects.

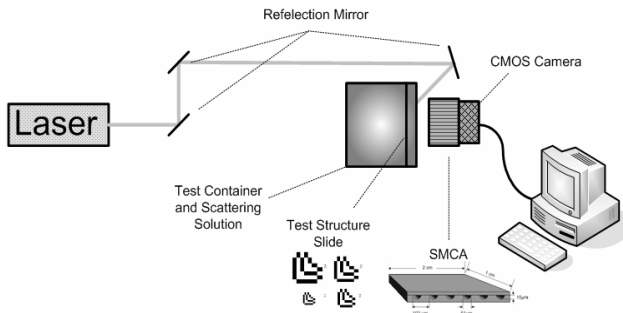


Figure 6. Angled illumination of the scattering medium

Thus the test structures can be seen as high absorption areas over this uniform illumination if the depth of the test structures is small enough that scattering after them is small.

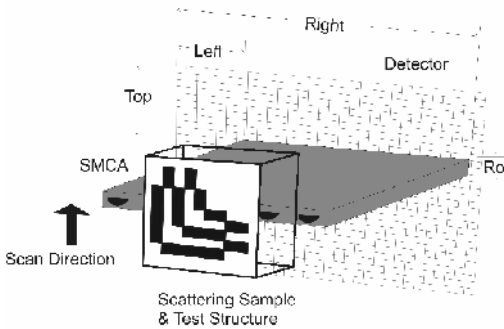


Figure 7. Scan of sample medium across SMCA

The SMCA is placed in front of an imaging array CMOS imaging array with a pixel size (5.2x5.2 microns) smaller than the collimating hole diameter of 51 microns. The photons reaching the pixels are filtered by the SMCA so that only those with a trajectory that lies within the collimating hole's acceptance angle reach the CMOS imager. Scanning the collimator along the sample is used to create a two-dimensional image from the linear array (see Figure 7).

IV. RESULTS

For these experiments, the test structure slide is placed at a distance of 3 mm, 2mm and 1mm back from the collimator side of the scattering medium. Figure 6 illustrates the setup used to illuminate the scattering medium from the same side of the camera. In Figure 8, a 2.5mm diameter Argon ion laser beam forms an angle of 54° with respect to the camera, and illuminates an SR=3x10¹²:1 scattering medium. The beam enters the scattering medium approximately 2 cm to the right of L shape phantoms placed within the medium. Because the light enters the scattering medium from the same surface as it is being viewed through, scattering that occurs from the point of entry until it forms an approximate sphere of illumination behind the sample is taken into account by our setup.

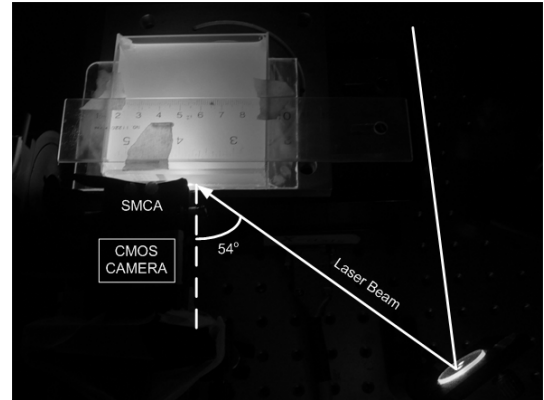


Figure 8. Angled illumination of the scattering medium

Figure 9 presents images obtained with the L shape sample at differing depths of one, two, and three millimeters in scattering media with SR values of 10¹⁰:1 to 10¹²:1 as calculated over 5 cm. For the silicon tunnels results, we can faintly resolve the largest 204µm-wide test structure lines at up to the 3mm depth and the maximum SR of 10¹²:1. At the 1mm depth, contrast and definition are improved and the presence of the smallest 51µm test structure can be detected. These results demonstrate that subsurface imaging of structures at depths up to 3 mm with sub-millimeter resolution is possible, even under high scattering levels that are typical to some bodily tissues [10].

Detection of very small features on the order of 51 µm is limited to depths shallower than 3 mm, which is surprising when considering that transillumination ADI has been shown successful at SR=8.9E9:1 over 5 cm. However, a 3 mm depth in such a medium only corresponds to SR=3.95:1 between the object and the surface. This degradation in imaging performance occurs because a collimated aligned light source is employed for transillumination, while backscatter illumination uses a randomly scattered source of light from within the scattering medium. Thus, backscatter ADI is much easier to set up, as the collimator does not need to be aligned to the laser source.

Measurements show that the light detected in between the collimator holes is 68% of the background light level detected within the collimator hole, indicating that scattered light is making its way through the tunnels and is emerging as diffuse, blurred light. Hence, removing this scattered light would significantly reduce background noise levels and significantly enhance the detectability of objects during imaging. Thus, the addition of an absorption coating to the SMCA tunnel sidewalls is expected to reduce the background scattered light level. A simple set of reflection tests were conducted to compare the reflectivity of silicon with a sputter-deposited carbon layer (see section III.A) versus an uncoated silicon surface. When comparing 200nm carbon-coated silicon with uncoated silicon, reflection is decreased from 40% to 20% under illumination by a 15° beam (relative to the perpendicular axis).

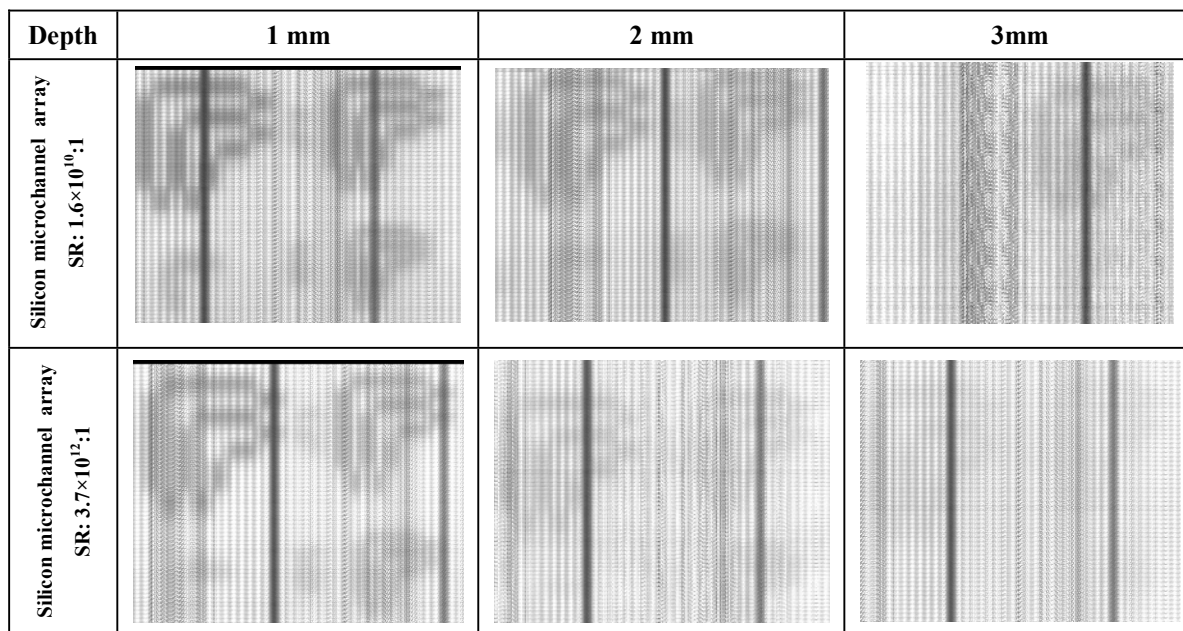


Figure 9. Comparison of the images captured by silicon *SMCA* in the various depth and two different scattering Ratio(SR).

For the 600nm carbon layer, reflection is decreased to 13%. When the beam angle is increased significantly so that it strikes the silicon surfaces at a shallow angle, reflection is increased dramatically for all three cases such that there is minimal difference between them. Thus, scan results comparing the silicon versus carbon coated tunnels show very little difference in contrast and feature definition. These results agree with our simple reflection tests, which indicate that our carbon coatings do not result in significant improvements in tunnel attenuation, especially at shallow angles.

These results suggest that the carbon sputtering process did not yield pure carbon coatings on the silicon surfaces. Thus, improved deposition of a pure carbon coating may yield the dramatic increase in tunnel attenuation that is desired.

V. CONCLUSION

In this paper the idea of backscattering angular domain imaging was proposed and the related experiments demonstrating its use were presented. This novel method of back scattering can give new areas of application to optical imaging, such as subcutaneous tissue mapping. The backscatter experiments were conducted using a modest laser beam angle of 54° to illuminate the sample, which can easily be applied to a wide range of objects and surfaces. Two dimensional phantom test structures have been successfully detected up to three millimeters deep in a highly scattering medium with a scattering ratio of over 10^{12} :1. In future work, two improvements will be explored to improve the image quality. First, the half circular collimators can be replaced by fully circular channels. Second, multiple lasers, each with a different

wavelength, along with image processing techniques, will be used and explored.

REFERENCES

- [1] Fartash Vasefi, Bozena Kaminska, Glenn H. Chapman, Paulman K.Y. Chan, "Angular Domain Imaging for Tissue Mapping", 2nd ASM - IEEE EMBS Conference on Bio, Micro and Nan- systems, January 15-18, 2006, San Francisco, USA.
- [2] Britton Chance, et al., "Optical Tomography and Spectroscopy of Tissue: Theory, Instrumentation, Model, and Human Studies II," Proceedings of the SPIE, vol. 2979, /, 1997.
- [3] J.R. Mourant, et. all., "Mechanisms of light scattering from biological cells relevant to noninvasive optical-tissue diagnostics," Appl.Opt., vol. 37, pp. 3586-93, 06/01. 1998.
- [4] T. Vodinh, "In-vivo Cancer-Diagnosis of the Esophagus Using Differential Normalized Fluorescence (DNF) Indexes," Lasers Surg.Med., vol. 16, pp. 41-47, 1995
- [5] J.C. Hebden and D.T. Delpy, "Enhanced time-resolved imaging with a diffusion model of photon transport," Opt.Lett., vol. 19, pp. 311-13, 03/01. 1994.
- [6] B.B. Das, K.M. Yoo and R.R. Alfano, "Ultrafast time-gated imaging in thick tissues: a step toward optical mammography," Opt.Lett., vol. 18, pp. 1092-4, 07/01. 1993.
- [7] A.F. Fercher, W. Drexler, C.K. Hitzenberger and T. Lasser, "Optical coherence tomography-principles and applications," Reports on Progress in Physics, vol. 66, pp. 239-303, 02/ 2003.
- [8] M.A. O'Leary, D.A. Boas, B. Chance and A.G. Yodh, "Experimental images of heterogeneous turbid media by frequency-domain diffusing-photon tomography," Opt.Lett., vol. 20, pp. 426-8, 03/01. 1995.
- [9] S.B. Colak, D.G. Papaioannou, G.W. 't Hooft, M.B. van der Mark, H. Schomberg, J.C.J. Paasschens, J.B.M. Melissen and N.A.A.J. van Asten, "Tomographic image reconstruction from optical projections in light-diffusing media," Appl.Opt., vol. 36, pp. 180-213, 01/01. 1997.
- [10] Glenn H. Chapman, Josna Rao, Ted Liu, Paulman K.Y. Chan, Fartash Vasefi, Bozena Kaminska, and Nick Pfeiffer, "Enhanced ADI in Turbid Medium using Gaussian Line Illumination", Proceedings of SPIE Volume: 6084, BIOS06, Jan 2006
- [11] J Beuthan et al., "IR-Diaphanoscopy in Medicine", *Medical Optical Tomography: Functional Imaging and Monitoring*, G. Muler et al. (eds), SPIE IS11, pp. 263-282, 1993.